The interaction between ORF18 and ORF30 is required for late gene transcription in Kaposi's sarcoma-associated herpesvirus

Angelica F Castañeda[a], and Britt A Glaunsinger[a,b,#]

[a] Department of Plant & Microbial Biology, University of California Berkeley, CA, USA

[b] Howard Hughes Medical Institute, Berkeley, CA, USA

[#]Corresponding Author: glaunsinger@berkeley.edu

Running title: Late gene expression requires ORF18-ORF30 interaction

Abstract

In the beta- and gammaherpesviruses, a specialized complex of viral transcriptional activators (vTAs) coordinate to direct expression of virus-encoded late genes, which are critical for viral assembly and whose transcription initiates only after the onset of viral DNA replication. The vTAs in Kaposi's sarcoma-associated herpesvirus (KSHV) are ORF18, ORF24, ORF30, ORF31, ORF34, and ORF66. While the general organization of the vTA complex has been mapped, the individual roles of these proteins, and how they coordinate to activate late gene promoters, remains largely unknown. Here, we performed a comprehensive mutational analysis of the conserved residues in ORF18, a highly interconnected vTA component. Surprisingly, the mutants were largely selective for disrupting the interaction with ORF30 but not the other three ORF18 binding partners. Furthermore, disrupting the ORF18-ORF30 interaction weakened the vTA complex as a whole, and an ORF18 point mutant that failed to bind ORF30 was unable

22 to complement an ORF18 null virus. Thus, contacts between individual vTAs are critical, as even
23 small disruptions in this complex result in profound defects in KSHV late gene expression.
24
25 **Importance**
26 Kaposi's sarcoma-associated herpesvirus (KSHV) is the etiologic agent of Kaposi's sarcoma and
27 other B-cell cancers and remains a leading cause of death in immunocompromised individuals.
28 A key step in the production of infectious virions is the transcription of viral late genes, which
29 generates capsid and structural proteins and requires the coordination of six viral proteins that
30 form a complex. The role of these proteins during transcription complex formation and the
31 importance of protein-protein interactions are not well understood. Here, we focused on a
32 central component of the complex, termed ORF18, and revealed that disruption of its
33 interaction with even a single component of the complex (ORF30) prevents late gene
34 expression and completion of the viral lifecycle. These findings underscore how individual
35 interactions between the late gene transcription components are critical for both the stability
36 and function of the complex.
37
38 **Introduction**
39 A broadly conserved feature of the lifecycle of dsDNA viruses is that replication of the
40 viral genome licenses transcription of a specific class of viral transcripts termed late genes.
41 There is an intuitive logic behind this coupling, as late genes encode proteins that participate in
42 progeny virion assembly and egress, and thus are not needed until newly synthesized genomes
43 are ready for packaging. Additionally, late gene transcription requires ongoing DNA replication,

44 and in the gammaherpesviruses Kaposi's sarcoma-associated herpesvirus (KSHV) and Epstein-
45 Barr virus (EBV) the increase in template abundance appears insufficient to explain the robust
46 transcription of late genes whose products are required in large amounts (1).

47 While the mechanisms underlying late gene activation can vary across viral families, in
48 the beta- and gammaherpesviruses, late gene promoters are strikingly minimalistic and
49 primarily consist of a modified TATA box (TATT) and ~10-15 base pairs of variable flanking
50 sequence (2–5). Despite this sequence simplicity, their transcription requires a dedicated set of
51 at least six conserved viral transcriptional activators (vTAs) whose precise roles are only
52 beginning to be uncovered. In KSHV, the vTAs are encoded by open reading frames (ORFs) 18,
53 24,30, 31, 34, and 66 (6–15). The best characterized of the vTAs is a viral TATA-binding protein
54 (TBP) mimic, encoded by ORF24 in KSHV, which binds both the late gene promoter and RNA
55 polymerase II (Pol II) (4, 8, 16, 17). Beyond the viral TBP mimic, the only other vTA with a
56 documented transcription-related function is pUL79 (homologous to KSHV ORF18) in human
57 cytomegalovirus (HCMV), which promotes transcription elongation at late times of infection
58 (18). Roles for the remaining vTAs remain largely elusive, although the KSHV ORF34 protein and
59 its murine cytomegalovirus (MCMV) homolog pM95 may function as hub proteins, as they
60 interact with numerous other vTAs (7, 9, 19). In addition to the six conserved vTAs, in EBV, the
61 kinase activity of BGLF4 (homologous to KSHV ORF36) also contributes to the expression of late
62 genes (20, 21).

63 Studies in both beta-and gammaherpesviruses indicate that the vTAs form a complex,
64 the general organization of which has been mapped in MCMV and KSHV (7, 9, 10, 19) (Figure
65 1A). Notably, several recent reports demonstrate that specific interactions between the vTAs

66 are critical for late gene transcription. In MCMV, mutation of conserved residues in pM91
67 (homologous to KSHV ORF30) that disrupt its interaction with pM79 (homologous to KSHV
68 ORF18) renders the virus unable to transcribe late genes (19). Similarly, the interaction
69 between KSHV ORFs 24 and 34 can be abrogated by a single amino acid mutation in ORF24
70 which prevents late gene transcription (9). Further delineating these contacts should provide
71 foundational information relevant to understanding vTA complex function.

72 The precise role of KSHV ORF18 in late gene transcription remains unknown, however it
73 is predicted to interact with four of the five other vTAs (ORFs 30, 31, 34, and 66), suggesting
74 that—like ORF34—it may play a central role in vTA complex organization (7, 9). Here, we
75 performed an interaction screen of ORF18 mutants to comprehensively evaluate the roles of its
76 conserved residues in mediating pairwise vTA binding. We reveal that ORF30 is particularly
77 sensitive to mutation in ORF18, enabling isolation of mutants that selectively abrogate this
78 interaction while retaining the contacts between ORF18 and the other vTAs. Disrupting the
79 ORF18-ORF30 interaction not only prevents KSHV late gene transcription, but also appears to
80 weaken assembly of the remaining vTA complex. These findings underscore the key role that
81 ORF18 plays in late gene transcription and suggest that disrupting just one of its interactions
82 has a destabilizing effect on the vTA complex as a whole.

83

84 **Results**

85 **ORF18 interacts with ORF30, ORF31, ORF34, and ORF66**

86 Previous work using a split luciferase-based interaction screen suggested that ORF18 is
87 highly interconnected with other viral late gene activators, as it interacted with the majority of

88 the proteins in the viral transcription pre-initiation complex (vPIC) (9). To independently
89 confirm the binding of ORF18 to ORFs 30, 31, 34, and 66 in the absence of other viral factors,
90 we assessed its ability to co-immunoprecipitate (co-IP) with each of these vTAs in transfected
91 HEK293T cells. Consistent with the screening data, ORF18-3xFLAG interacted robustly with C-
92 terminal 2xStrep-tagged versions of ORF30, ORF31, and ORF66 (Figure 1B, D, E). Furthermore,
93 we consistently observed that the expression of ORF30 was higher when co-expressed with
94 ORF18 than when transfected with vector control, suggesting that ORF18 may stabilize ORF30
95 (Figure 1B). Although ORF18-3xFLAG did not interact with ORF34 tagged on its C-terminus, the
96 interaction was recovered upon moving the 2xStrep tag to the N-terminus of ORF34 (Figure 1C).
97

98 **An interaction screen of ORF18 mutants reveals the role of conserved residues in interactions**
99 **with the other vTAs**

100 To evaluate the importance of the interaction between ORF18 and its individual vTA
101 contacts, we aimed to identify point mutations that disrupted binding to individual vTAs but did
102 not destroy the integrity of the complex. Since the late gene vTA complex is conserved across
103 the beta- and gammaherpesviruses we reasoned that the individual points of contact might
104 depend on conserved amino acid residues. We performed a multiple sequence alignment
105 between KSHV ORF18 and its homologs in five other beta- and gamma herpesviruses (MHV68
106 ORF18, HCMV pUL79, MCMV pM79, EBV BVLF1, and BHV ORF18) using MUSCLE (22). The
107 sequence alignment revealed 25 single conserved residues, including six pairs of adjacent
108 conserved residues, which are depicted in Figure 2A as a schematic of the primary structure of
109 ORF18 showing the positions of conserved residues. We mutated each of the 25 conserved

110 residues to alanine in ORF18-3xFLAG and made double alanine mutations in the six cases of
111 adjacent conserved residues (Figure 2A). Each of these 31 mutants was screened individually
112 for the ability to interact with ORFs 30, 31, and 66 by co-IP followed by western blot (data not
113 shown). To account for differences in expression between the ORF18 mutants, we calculated
114 the co-IP efficiency of each of the mutants, as described in the methods. These data were used
115 to generate a heat map, which displays the pair-wise interaction efficiencies on a color scale
116 where lighter blocks represent reduced binding and darker blocks represents increased binding
117 relative to WT (Figure 2B). Overall, the data revealed that ORF30 was the most sensitive to
118 mutations in ORF18, as 24 out of the 31 mutants displayed reduced or no binding. ORF31
119 showed variable sensitivity to ORF18 mutation (with some mutants even increasing the
120 interaction efficiency), while the ORF66-ORF18 interaction was relatively refractory to the
121 ORF18 point mutations (Figure 2B).

122 We focused on the six ORF18 mutants that exhibited <10% co-IP efficiency, relative to
123 WT, with any vTA in our initial screen (L29A, E36A, L151A, W170A, E36A_L37A, and
124 W170A_G171A; highlighted in red in Figure 2A). These were re-screened 3-4 independent times
125 in co-IP assays with vTA components ORFs 30, 31, 34, and 66, and the co-IP efficiencies were
126 calculated as described in the methods then plotted relative to values obtained for WT ORF18
127 (Figure 3A-D). All six of these ORF18 mutants had severe defects in their ability to co-IP ORF30,
128 but none were consistently different than WT ORF18 for interaction with ORFs 31, 34, and 66
129 (Figure 3B-D). Among the six mutants, ORF18^{E36A_L37A} and ORF18^{W170A_G171A} showed no
130 detectable binding to ORF30, with ORF18^{E36A_L37A} retaining near-WT levels of interaction with
131 the remaining vTAs.

132 **ORF18 point mutants that weaken the interaction between ORF18 and ORF30 have a reduced**
133 **capacity to activate the K8.1 late gene promoter**

134 A reporter assay has been developed in which the co-expression of the six individual
135 vTAs can specifically activate a KSHV (or EBV) late gene promoter in transfected HEK293T cells
136 (9, 10). We used this assay as an initial proxy for the ability of the six ORF18 mutants described
137 above to activate late gene transcription. HEK293T cells were co-transfected with each of the
138 vTAs, including either WT or mutant ORF18, and firefly luciferase reporter plasmids driven by
139 either the late K8.1 promoter or, as a control, the early ORF57 promoter (Figure 4A). A plasmid
140 containing constitutively expressed Renilla luciferase was co-transfected with each sample to
141 normalize for transfection efficiency. As expected, inclusion of WT ORF18 with the remaining
142 vTA complex resulted in specific activation of the K8.1 late promoter, but not of the early
143 ORF57 promoter (Figure 4B). ORF18 mutants L29A, E36A, and L151A modestly reduced
144 activation of the late promoter, whereas more significant defects were observed with mutants
145 W170A, E36A_L37A, and W170A_G171A (Figure 4B). Although ORF18^{W170A_G171A} had the most
146 pronounced transcriptional defect, this mutant showed somewhat more variability than
147 ORF18^{E36A_L37A} in its interactions with the other vTA components (Figures 3 & 4). Thus, we
148 considered ORF18^{E36A_L37A} to be the top candidate for selectively analyzing the importance of
149 the ORF18-ORF30 interaction for KSHV late gene transcription.

150

151 **The interaction between ORF18 and ORF30 affects assembly of the vTA complex**

152 The transcriptional defect of the ORF18^{E36A_L37A} mutant in the reporter assay could be
153 due to a defect in assembly of the complex or due to defects in downstream events. To

154 distinguish between these possibilities, WT or mutant ORF18-3xFLAG was co-transfected into
155 HEK293T cells with each of the other Strep-tagged vTAs. We then performed an α-FLAG IP,
156 revealing that purification of WT ORF18 led to co-IP of the complete vTA complex including Pol
157 II, which has been shown to interact with ORF24 in KSHV (8) (Figure 5). We noted that in this
158 assay ORF18^{E36A_L37A} was more weakly expressed than WT ORF18, so to compare complex
159 formation with equivalent amounts of each protein, we titrated down the amount of WT ORF18
160 to match the levels of ORF18^{E36A_L37A}. Similar to our observation in a pairwise co-IP (Figure 1B),
161 the ORF30 protein abundance decreased as the expression of ORF18 was reduced (Figure 5);
162 however, the complete vTA complex still co-purified even with reduced levels of WT ORF18
163 (Figure 5). Notably, the vTA complex was recovered at lower levels in the presence of
164 ORF18^{E36A_L37A}. When imaged at a longer exposure, all of the vTAs, with the exception of ORF30,
165 remained associated with ORF18^{E36A_L37A} (Figure 5, far right panel). Thus, the selective loss of
166 the ORF18-ORF30 interaction may reduce the overall stability of the vTA complex.
167

168 **The interaction between ORF18 and ORF30 is crucial for late gene transcription**

169 Next, to characterize the effect of ORF18^{E36A_L37A} on the viral replication cycle, we tested
170 the ability of this mutant to complement the late gene expression defect of a KSHV mutant
171 lacking ORF18 (18.stop) (6). The renal carcinoma cell line iSLK harbors the virus (either WT or
172 18.stop) in a latent state, which can be reactivated upon expression of the doxycycline-
173 inducible major lytic transactivator RTA and treatment with sodium butyrate. Using lentiviral
174 transduction, we generated stable, doxycycline-inducible versions of the 18.stop iSLK cells
175 expressing either ORF18-3xFLAG or ORF18^{E36A_L37A}-3xFLAG (18.stop.ORF18^{WT} and

176 18.stop.ORF18^{E36A_L37A}, respectively). The cells were assayed 72 hours post lytic reactivation for
177 their ability to replicate DNA, express early and late proteins, and produce progeny virions.
178 Although we observed a modest decrease of viral DNA replication in the 18.stop cells, as
179 measured by qPCR, upon complementation with either WT ORF18 or ORF18^{E36A_L37A}, the levels
180 of DNA replication were not significantly different from iSLK cells infected with WT KSHV (Figure
181 6A). Notably, the 18.stop.ORF18^{E36A_L37A} cell line expressed more ORF18 than the
182 18.stop.ORF18^{WT} cell line, in contrast to the reduced expression of the mutant in HEK293T cells
183 (Figure 6B, compare to levels in Figure 5). However, while both reactivated 18.stop.ORF18^{WT}
184 and 18.stop.ORF18^{E36A_L37A} cell lines expressed equivalent levels of the ORF59 early protein,
185 only 18.stop.ORF18^{WT} was able to rescue expression of the K8.1 late gene (Figure 6B).
186 We then evaluated the level of KSHV virion production from the parental WT KSHV-
187 infected iSLK cells, as well as from the 18.stop, 18.stop.ORF18^{WT}, and 18.stop.ORF18^{E36A_L37A} cell
188 lines using a supernatant transfer assay. KSHV produced from iSLK cells contains a constitutively
189 expressed GFP, enabling quantitation of infected recipient cells by flow cytometry (23).
190 Consistent with its late gene expression defect, neither the 18.stop nor the
191 18.stop.ORF18^{E36A_L37A} cell lines were able to produce progeny virions, whereas virion
192 production in the 18.stop.ORF18^{WT} cells was indistinguishable from the WT KSHV-infected iSLK
193 cells (Figure 6C). Collectively, these data demonstrate that the specific interaction between
194 ORF18 and ORF30 is essential for late gene expression and virion production during KSHV
195 infection.
196
197

198 **The analogous mutation in HCMV pUL79 disrupts its interaction with pUL91**

199 As shown in Figure 7A, the E36_L37 residues are conserved across the beta- and
200 gammaherpesvirus ORF18 homologs. To determine whether these amino acids are similarly
201 important in a betaherpesvirus, we engineered the corresponding double mutation in HCMV
202 pUL79 (pUL79^{E48A_L49A}-3xFLAG). Similar to our observation with KSHV ORF30, HCMV pUL91
203 protein expression was significantly decreased in the absence of its WT pUL79 binding partner
204 (Figure 7B). This is consistent with the idea that pUL79 binding stabilizes pUL91. Furthermore,
205 in co-IP assays we detected a robust interaction between pUL79 and pUL91, which was
206 impaired in the presence of pUL79^{E48A_L49A}, even when we accounted for the expression level
207 differences of pUL91 (Figure 7B). This suggests that the overall protein-protein interface may be
208 conserved in the analogous ORF18-ORF30 interaction across the beta- and
209 gammaherpesviruses.

210

211 **Discussion**

212 Elucidating the architecture of the six-member vPIC complex is central to understanding
213 the mechanism underlying viral late gene expression in beta- and gammaherpesviruses.
214 Although their functions are largely unknown, each of these viral transcription regulators is
215 essential for late gene promoter activation and evidence increasingly suggests that their ability
216 to form a complex is crucial for transcriptional activity (9, 10, 19). Here, we reveal that selective
217 disruption of an individual protein-protein contact between KSHV ORF18 and ORF30 within the
218 vPIC is sufficient to abrogate late gene transcription and virion production in infected cells,
219 emphasizing the sensitivity of the complex to organizational perturbation.

220 We selected ORF18 for mutational screening due to its ability to form pairwise
221 interactions with the majority of other vPIC components, which suggested that it might serve as
222 an organizational hub for vPIC assembly, similar to what has been proposed for ORF34 (7, 9).
223 However, the 31 tested mutants of ORF18 revealed that conserved residues across the length
224 of the protein are extensively—and largely selectively— required for ORF30 binding. This is in
225 contrast to the interaction between the vPIC components ORF24 and ORF34, where the
226 interaction can be localized to a 17 amino acid stretch of ORF24 (9). The observation that the
227 majority of the ORF18 point mutations that disrupt the interaction with ORF30 do not affect its
228 binding to ORFs 31, 34, and 66 indicates that these mutations do not significantly alter the
229 overall folding or structure of ORF18. In MCMV, the organization of the vTA complex is similar
230 to KSHV, except that pM92 (homologous to KSHV ORF31) interacts with pM87 (homologous to
231 KSHV ORF24), whereas in KSHV this interaction is bridged through ORF34 (19). Our data
232 complement recent findings in MCMV, in which mutations of the ORF30 homolog (pM91) that
233 perturb the interaction with the ORF18 homolog (pM79) similarly cause a defect in the
234 expression of late genes (19). Thus, mutations that disrupt the ORF18-ORF30 protein-protein
235 interface in either protein cause the same phenotype.

236 The ORF18-ORF30 interaction appears sensitive to single amino acid changes in the
237 protein-protein interface. The ORF18^{E36A_L37A} mutation does not impair binding to its other vPIC
238 partners in pairwise co-IP experiments and ORF30 does not engage in pairwise interactions with
239 vPIC components other than ORF18 (7, 9). It is therefore notable that the efficiency of the vPIC
240 complex assembly is reduced in HEK293T cells in the presence of the ORF18^{E36A_L37A} mutant,
241 suggesting that the ORF18-ORF30 interaction contributes to the stability of the complex as a

242 whole. The interaction between ORF18 and ORF30 may change the conformation of ORF18,
243 allowing it to interact more strongly with the other vTAs.

244 We observed that ORF30 protein expression was consistently higher in the presence of
245 WT ORF18 or ORF18 mutants that retained ORF30 binding, suggesting that ORF18 helps
246 stabilize ORF30. *In silico* protein stability prediction studies have suggested that protein stability
247 is in part affected by protein length, where proteins that are less than 100 amino acids tend to
248 be less stable (24, 25). One explanation for the higher expression of ORF30 in the presence of
249 ORF18 could therefore be that the 77 amino acid ORF30 is protected from degradation by
250 ORF18. Another possibility is that ORF18 helps keep ORF30 correctly folded—this has been
251 proposed as a mechanism that stabilizes proteins which have interaction partners (26). The
252 interaction-induced stability of a protein often correlates with the relative concentration of its
253 binding partners (26), as we observed when we titrated down the amount of ORF18 in the
254 context of the complete vTA complex. A similar observation has been made between KSHV
255 proteins ORF36 and ORF45, where ORF36 was dependent on the interaction with ORF45 for
256 stabilization (27). We did not observe a similar correlation with levels of the other ORF18-
257 associated vPIC proteins, and thus their stability may not require protective interactions. We
258 also observed a stabilizing effect of pUL79 on pUL91, indicating this may be a conserved feature
259 of this interaction in other beta- and gammaherpesviruses.

260 The fact that the late gene expression defect of the ORF18^{E36A_L37A} mutant is
261 exacerbated in the context of the virus, compared to in the plasmid promoter activation assay,
262 likely reflects the fact that the plasmid assay measures basal promoter activation but misses
263 other regulatory components of this cascade. For example, the origin of lytic replication is

264 required *in cis* for late gene expression in related gammaherpesviruses (3, 28) and the reporter
265 assay does not capture the important contribution of viral DNA replication towards late gene
266 expression. This may explain why some mutants that are defective for ORF30 binding (e.g.
267 L29A, E36A, L151A) retain partial plasmid promoter activity; perhaps some weak binding
268 between ORF18 and ORF30 enables basal activation of the promoter in a context where the
269 vPIC components are overexpressed. Alternatively, some of the mutations may cause ORF18 to
270 bind to ORF30 more transiently, but their vPIC interaction becomes stabilized in the presence of
271 a late gene promoter.

272 In summary, the absence of late gene transcription in the KSHV ORF18.stop-infected
273 cells complemented with ORF18^{E36A_L37A} may derive from a cascade of phenotypes: the failure
274 to recruit ORF30 to the vPIC, the ensuing reduction in the efficiency of overall vPIC complex
275 assembly, and the reduced stability of ORF30 (if it also has additional vPIC-independent
276 functions). Ultimately, generating antibodies that recognize the endogenous KSHV vPIC
277 components will enable these phenotypes to be explored further during infection. In addition,
278 information about the 3-dimensional structure of the vPIC would significantly enhance our
279 understanding of this unique transcription complex, as it is becoming increasingly clear that
280 even small disruptions to the complex dramatically impact completion of the viral lifecycle.

281

282 **Materials and Methods**

283 **Plasmids and Plasmid construction**

284 To generate ORF18-3xFLAG pCDNA4, ORF18 was subcloned into the BamHI and NotI sites of
285 pCDNA-3xFLAG. The point mutations in ORF18 were generated using two primer site-directed

286 mutagenesis with Kapa HiFi polymerase (Roche) with primers 1-62 listed in Table 1. All
287 subsequent plasmids described below were generated using InFusion cloning (Clontech) unless
288 indicated otherwise. To generate plasmid pLVX-TetOneZeo, zeocin resistance was PCR amplified
289 out of plasmid pLJM1-EGFP-Zeo with primers 63/64 (Table 1) and used to replace the
290 puromycin resistance in pLVX-TetOne^{TM}-Puro (Clontech) using the AvrII and MluI restriction
291 sites. To generate pLVX-TetOneZeo-ORF18^{WT}-3xFLAG and pLVX-TetOneZeo-ORF18^{E36A_L37A}-
292 3xFLAG, ORF18^{WT}-3xFLAG and ORF18^{E36_37A}-3xFLAG were PCR amplified from each respective
293 pCDNA4 plasmid using primers 71/72 and inserted into the EcoRI and BamHI sites of pLVX-
294 TetOne-Zeo. To generate UL79-3xFLAG pCDNA4 and UL91-2xStrep pCDNA4, UL79 was PCR
295 amplified with primers 67/68 (Table 1) and UL91 was PCR amplified with primers 69/70 (Table
296 1) from HCMV Towne strain, which was kindly provided by Dr. Laurent Coscoy, and cloned into
297 the BamHI and NotI sites of 3xFLAG (Cterm) pCDNA4 or 2xStrep (Cterm) pCDNA4. UL79^{E48A_L49A}
298 was generated with two primer site-directed mutagenesis using Kapa HiFi polymerase with
299 primers 73/74 (Table 1). To make 2xStrep-ORF34 pCDNA4, ORF34 was PCR amplified from
300 ORF34-2xStrep pCDNA4 with primers 65/66 and cloned into the NotI and XbaI sites of 2xStrep
301 (Nterm) pCDNA4. Plasmid K8.1 Pr pGL4.16 contains the minimal K8.1 promoter and ORF57 Pr
302 pGL4.16 contains a minimal ORF57 early gene promoter and have been described previously
303 (9). Plasmids ORF18-2xStrep pCDNA4, ORF24-2xStrep pCDNA4, ORF30-2xStrep pCDNA4, ORF31-
304 2xStrep pCDNA4, ORF34-2xStrep pCDNA4, and ORF66-2xStrep pCDNA4 have been previously
305 described (8). Plasmid pRL-TK (Promega) was kindly provided by Dr. Russel Vance. Lentiviral
306 packaging plasmids psPAX2 (Addgene plasmid # 12260) and pMD2.G (Addgene plasmid #
307 12259) were gifts from Dr. Didier Trono.

308 **Cells and transfections**

309 HEK293T cells (ATCC CRL-3216) were maintained in DMEM supplemented with 10% FBS
310 (Seradygm). The iSLK renal carcinoma cell line harboring the KSHV genome on the bacterial
311 artificial chromosome BAC16 and a doxycycline-inducible copy of the KSHV lytic transactivator
312 RTA (iSLK-BAC16) has been described previously (23). iSLK-BAC16-ORF18.stop cells that contain
313 a stop mutation in ORF18 were kindly provided by Dr. Ting-Ting Wu (6). iSLK-BAC16 and iSLK-
314 BAC16-ORF18.stop were maintained in DMEM supplemented with 10% FBS, 1 mg/ml
315 hygromycin, and 1 μg/ml puromycin (iSLK-BAC16 media). iSLK-BAC16-ORF18.stop cells were
316 complemented by lentiviral transduction with ORF18^{WT}-3xFLAG or ORF18^{E36A_L37A}-3xFLAG. To
317 generate the lentivirus, HEK293T cells were co-transfected with pLVX-TetOneZeo-ORF18^{WT}-
318 3xFLAG or pLVX-TetOneZeo-ORF18^{E36A_L37A}-3xFLAG along with the packaging plasmids pMD2.G
319 and psPAX2. After 48h, the supernatant was harvested and syringe-filtered through a 0.45 μm
320 filter (Millipore). The supernatant was diluted 1:2 with DMEM and polybrene was added to a
321 final concentration of 8 μg/ml. 1 x 10^6 iSLK-BAC16-ORF18.stop freshly trypsinized cells were
322 spinfected in a 6-well plate for 2 h at 500 x *g*. After 24 h the cells were expanded to a 10 cm
323 tissue culture plate and selected for 2 weeks in iSLK-BAC16 media supplemented with 325
324 μg/ml zeocin (Sigma). For DNA transfections, HEK293T cells were plated and transfected after
325 24 h at 70% confluency with PolyJet (SignaGen).

326

327 **Immunoprecipitation and western blotting**

328 Cell lysates were prepared 24 h after transfection by washing and pelleting cells in cold
329 PBS, then resuspending the pellets in lysis buffer [50 mM Tris-HCl pH 7.4, 150 mM NaCl, 1mM

330 EDTA, 0.5% NP-40, and protease inhibitor (Roche)] and rotating them at 4 °C for 30 minutes.
331 Lysates were cleared by centrifugation at 21,000 x *g* for 10 min, then 1 mg (for pairwise
332 interaction IPs) or 2 mg (for the entire late gene complex IPs) of lysate was incubated with pre-
333 washed M2 anti-FLAG magnetic beads (Sigma) overnight. The beads were washed 3x for 5 min
334 each with IP wash buffer [50 mM Tris-HCl pH 7.4, 150 mM NaCl, 1mM EDTA, 0.05% NP-40] and
335 eluted with 2x Laemmli sample buffer (BioRad).

336 Lysates and elutions were resolved by SDS-PAGE and western blotted in TBST (Tris-
337 buffered saline, 0.2% Tween 20) using the following primary antibodies: Strep-HRP (Millipore,
338 1:2500); rabbit anti-FLAG (Sigma, 1:3000); mouse anti-FLAG (Sigma, 1:1000); rabbit anti-
339 Vinculin (Abcam, 1:1000); mouse anti-GAPDH (Abcam, 1:1000); mouse anti-Pol II CTD clone
340 8WG16 (Abcam, 1:1000); rabbit anti-K8.1 (1:10000); rabbit anti-ORF59 (1:10000). Rabbit anti-
341 ORF59 and anti-K8.1 was produced by the Pocono Rabbit Farm and Laboratory by immunizing
342 rabbits against MBP-ORF59 or MBP-K8.1 [gifts from Denise Whitby (29)]. Following incubation
343 with primary antibodies, the membranes were washed with TBST and incubated with the
344 appropriate secondary antibody. The secondary antibodies used were the following: goat anti-
345 mouse-HRP (1:5000, Southern Biotech) and goat anti-rabbit-HRP (1:5000, Southern Biotech).

346 The co-IP efficiency for the pairwise interactions was quantified from the western blot
347 images using Image Lab software (BioRad). The band intensity for the both the Strep-tagged
348 ORF and ORF18^{WT}-3xFLAG or ORF18^{Mu}-3xFLAG was calculated for the IP lanes of the western
349 blot. The ratio of the band intensity of Strep-tagged ORF to ORF18^{Mu}-3xFLAG was divided by the
350 ratio of Strep-tagged ORF to ORF18^{WT}-3xFLAG to generate a co-IP efficiency for each ORF18^{Mu}
351 relative to the co-IP efficiency of ORF18^{WT}.

352 **Virus Characterization**

353 For reactivation studies, 1 x 10^6 iSLK cells were plated in 10 cm dishes for 16 h, then
354 induced with 1 μg/ml doxycycline and 1 mM sodium butyrate for an additional 72 h. To
355 determine the fold DNA induction in reactivated cells, the cells were scraped and triturated in
356 the induced media, and 200 μl of the cell/supernatant suspension was treated overnight with
357 80 μg/ml proteinase K (Promega) in 1x proteinase K digestion buffer (10 mM Tris-HCl pH 7.4,
358 100 mM NaCl, 1 mM EDTA, 0.5% SDS) after which DNA was extracted using a Quick-DNA
359 Miniprep kit (Zymo). Viral DNA fold induction was quantified by qPCR using iTaq Universal SYBR
360 Green Supermix (BioRad) on a QuantStudio3 Real-Time PCR machine with primers 75/76 (Table
361 1) for the KSHV ORF59 promoter and normalized to the level of GAPDH promoter with primers
362 77/78 (Table 1).

363 Infectious virion production was determined by supernatant transfer assay. Supernatant
364 from induced iSLK cells was syringe-filtered through a 0.45 μm filter and diluted 1:2 with
365 DMEM, then 2 mL of the supernatant was spinoculated onto 1 x 10^6 freshly trypsinized
366 HEK293T cells for 2 h at 500 x *g*. After 24 h, the media was aspirated, the cells were washed
367 once with cold PBS and crosslinked in 4% PFA (Ted Pella) diluted in PBS. The cells were pelleted,
368 resuspended in PBS, and a minimum of 50,000 cells/sample were analyzed on a BD Accuri 6
369 flow cytometer. The data were analyzed using FlowJo (30).

370

371 **Late Gene Reporter Assay**

372 HEK293T cells were plated in 6-well plate and each well was transfected with 900 ng of DNA
373 containing 125 ng each of pcDNA4 ORF18-3xFLAG or ORF18^{Mu}-3xFLAG, ORF24-2xStrep, ORF30-

374 2xStrep, ORF31-2xStrep, 2xStrep-ORF34, ORF66-2xStrep, and either K8.1 Pr pGL4.16 or ORF57
375 Pr pGL4.16, along with 25 ng of pRL-TK as an internal transfection control. After 24 h, the cells
376 were rinsed once with PBS, lysed by rocking for 15 min at room temperature in 500 μl of
377 Passive Lysis Buffer (Promega), and clarified by centrifuging at 21,000 x *g* for 2 min. 20 μl of the
378 clarified lysate was added in triplicate to a white chimney well microplate (Greiner bio-one) to
379 measure luminescence on a Tecan M1000 microplate reader using a Dual Luciferase Assay Kit
380 (Promega). The firefly luminescence was normalized to the internal Renilla luciferase control for
381 each transfection.
382
383 **Acknowledgements**
384 We thank all members of the Glaunsinger and Coscoy labs, in particular Matthew R
385 Gardner, for their helpful suggestions and critical reading of the manuscript. This material is
386 based upon work supported by the National Science Foundation Graduate Research Fellowship
387 under Grant No. DGE 1752814 and UC Berkeley Chancellor's Fellowship awarded to A.C. B.G. is
388 an investigator of the Howard Hughes Medical Institute. This research was also supported by
389 NIH R01AI122528 to B.G.
390
391 **References**
392 1. Li D, Fu W, Swaminathan S. 2018. Continuous DNA replication is required for late gene
393 transcription and maintenance of replication compartments in gammaherpesviruses.
394 PLoS Pathog 14:1–25.
395 2. Serio TR, Cahill N, Prout ME, Miller G. 1998. A functionally distinct TATA box required for

396 late progression through the Epstein-Barr virus life cycle. J Virol 72:8338–8343.

397 3. Tang S, Yamanegi K, Zheng Z-M. 2004. Requirement of a 12-base-pair TATT-containing
398 sequence and viral lytic DNA replication in activation of the Kaposi's sarcoma-associated
399 herpesvirus K8.1 late promoter. J Virol 78:2609–2614.

400 4. Wong-Ho E, Wu TT, Davis ZH, Zhang BQ, Huang J, Gong H, Deng HY, Liu FY, Glaunsinger B,
401 Sun R. 2014. Unconventional Sequence Requirement for Viral Late Gene Core Promoters
402 of Murine Gammaherpesvirus 68. J Virol 88:3411–3422.

403 5. Djavadian R, Hayes M, Johannsen E. 2018. CAGE-seq analysis of Epstein-Barr virus lytic
404 gene transcription: 3 kinetic classes from 2 mechanisms. PLoS Pathog 14:1–26.

405 6. Gong D, Wu NC, Xie Y, Feng J, Tong L, Brulois KF, Luan H, Du Y, Jung JU, Wang C -y., Kang
406 MK, Park N-H, Sun R, Wu T-T. 2014. Kaposi's Sarcoma-Associated Herpesvirus ORF18 and
407 ORF30 Are Essential for Late Gene Expression during Lytic Replication. J Virol 88:11369–
408 11382.

409 7. Nishimura M, Watanabe T, Yagi S, Yamanaka T, Fujimuro M. 2017. Kaposi's sarcoma-
410 associated herpesvirus ORF34 is essential for late gene expression and virus production.
411 Sci Rep 7:1–12.

412 8. Davis ZH, Verschueren E, Jang GM, Kleffman K, Johnson JR, Park J, Shales M, Dollen J Von,
413 Maher MC, Johnson T, Newton W, Ja S, Horner J, Hernandez RD, Krogan NJ, Glaunsinger
414 B a. 2015. Global Mapping of Herpesvirus-Host Protein Complexes Reveals a
415 Transcription Strategy for Late Genes. Mol Cell 57:349–360.

416 9. Davis ZH, Hesser CR, Park J, Glaunsinger A. 2016. Associated Herpesvirus Late Gene
417 Transcription Factor Complex Is Essential for Viral Late Gene Expression. J Virol 90:599–

418 604.

419 10. Aubry V, Mure F, Mariame B, Deschamps T, Wyrwicz LS, Manet E, Gruffat H. 2014.
420 Epstein-Barr Virus Late Gene Transcription Depends on the Assembly of a Virus-Specific
421 Preinitiation Complex. J Virol 88:12825–12838.

422 11. Wu T-T, Park T, Kim H, Tran T, Tong L, Martinez-Guzman D, Reyes N, Deng H, Sun R. 2009.
423 ORF30 and ORF34 are essential for expression of late genes in murine gammaherpesvirus
424 68. J Virol 83:2265–2273.

425 12. Arumugaswami V, Wu T-T, Martinez-Guzman D, Jia Q, Deng H, Reyes N, Sun R. 2006.
426 ORF18 is a transfactor that is essential for late gene transcription of a gammaherpesvirus.
427 J Virol 80:9730–9740.

428 13. Jia Q, Wu T-T, Liao H-I, Chernishof V, Sun R. 2004. Murine gammaherpesvirus 68 open
429 reading frame 31 is required for viral replication. J Virol 78:6610–6620.

430 14. Brulois K, Wong L-Y, Lee H-R, Sivadas P, Ensser A, Feng P, Gao S-J, Toth Z, Jung JU. 2015.
431 Association of Kaposi's Sarcoma-Associated Herpesvirus ORF31 with ORF34 and ORF24 Is
432 Critical for Late Gene Expression. J Virol 89:6148–54.

433 15. Wong E, Wu T-T, Reyes N, Deng H, Sun R. 2007. Murine gammaherpesvirus 68 open
434 reading frame 24 is required for late gene expression after DNA replication. J Virol
435 81:6761–6764.

436 16. Gruffat H, Kadjouf F, Mariame B, Manet E. 2012. The Epstein-Barr Virus BcRF1 Gene
437 Product Is a TBP-Like Protein with an Essential Role in Late Gene Expression. J Virol
438 86:6023–6032.

439 17. Wyrwicz LS, Rychlewski L. 2007. Identification of Herpes TATT-binding protein. Antiviral

440 Res 75:167–172.

441 18. Perng Y-C, Campbell JA, Lenschow DJ, Yu D. 2014. Human cytomegalovirus pUL79 is an
442 elongation factor of RNA polymerase II for viral gene transcription. PLoS Pathog
443 10:e1004350.

444 19. Pan D, Han T, Tang S, Xu W, Bao Q, Sun Y, Xuan B, Qian Z. 2018. Murine Cytomegalovirus
445 Protein pM91 Interacts with pM79 and Is Critical for Viral Late Gene Expression. J Virol
446 JVI.00675-18.

447 20. El-Guindy A, Lopez-Giraldez F, Delecluse HJ, McKenzie J, Miller G. 2014. A Locus
448 Encompassing the Epstein-Barr Virus bglf4 Kinase Regulates Expression of Genes
449 Encoding Viral Structural Proteins. PLoS Pathog 10:e1004307.

450 21. McKenzie J, Lopez-Giraldez F, Delecluse HJ, Walsh A, El-Guindy A. 2016. The Epstein-Barr
451 Virus Immunoevasins BCRF1 and BPLF1 Are Expressed by a Mechanism Independent of
452 the Canonical Late Pre-initiation Complex. PLoS Pathog 12:1–32.

453 22. Edgar RC. 2004. MUSCLE: Multiple sequence alignment with high accuracy and high
454 throughput. Nucleic Acids Res 32:1792–1797.

455 23. Brulois KF, Chang H, Lee a. S-Y, Ensser a., Wong L-Y, Toth Z, Lee SH, Lee H-R, Myoung J,
456 Ganem D, Oh T-K, Kim JF, Gao S-J, Jung JU. 2012. Construction and Manipulation of a
457 New Kaposi's Sarcoma-Associated Herpesvirus Bacterial Artificial Chromosome Clone. J
458 Virol 86:9708–9720.

459 24. Dill KA. 1985. Theory for the Folding and Stability of Globular Proteins. Biochemistry
460 24:1501–1509.

461 25. White SH. 1992. Amino acid preferences of small proteins. J Mol Biol 227:991–995.

462 26. Dixit PD, Maslov S. 2013. Evolutionary Capacitance and Control of Protein Stability in
463 Protein-Protein Interaction Networks. PLoS Comput Biol 9 (4): e1003023.
464 27. Avey D, Tepper S, Pifer B, Bahga A, Williams H, Gillen J, Li W, Ogden S. 2016. Discovery of
465 a Coregulatory Interaction between Kaposi ' s Sarcoma- Associated Herpesvirus ORF45
466 and the Viral Protein Kinase ORF36. J Virol 90:5953–5964.
467 28. Djavadian R, Chiu YF, Johannsen E. 2016. An Epstein-Barr Virus-Encoded Protein Complex
468 Requires an Origin of Lytic Replication In Cis to Mediate Late Gene Transcription. PLoS
469 Pathog 12:1–25.
470 29. Labo N, Miley W, Marshall V, Gillette W, Esposito D, Bess M, Turano A, Uldrick T,
471 Polizzotto MN, Wyvill KM, Bagni R, Yarchoan R, Whitby D. 2014. Heterogeneity and
472 Breadth of Host Antibody Response to KSHV Infection Demonstrated by Systematic
473 Analysis of the KSHV Proteome. PLoS Pathog 10(3): e1004046.
474 30. Gardner MR, Glaunsinger BA. 2018. crossm Kaposi ' s Sarcoma-Associated Herpesvirus
475 ORF68 Is a DNA Binding Protein Required for Viral Genome Cleavage and 92:1–13.
476
477
478 **Figure 1**
479 ORF18 interacts with ORFs 30, 31, 34, and 66. (A) Diagram of vTA interactions in KSHV from (9).
480 (B-E) HEK293T cells were transfected with the indicated vTA plasmids, then subjected to co-IP
481 using α-FLAG beads followed by western blot analysis with the indicated antibody to detect
482 ORF18 and either ORF30 (*B*), ORF34 (*C*), ORF31 (*D*), and ORF66 (*E*). Input represents 2.5% of the
483 lysate used for co-IP. Vinculin served as a loading control.

484 **Figure 2**

485 ORF18 mutant screen for interactions with ORFs 30, 31, and 66. (A) Diagram depicting the
486 conserved residues in KSHV ORF18 in a MUSCLE alignment with MHV68 ORF18, EBV BVLF1,
487 HCMV pUL79, MCMV pUL79, and BHV4 ORF18. Red color denotes amino acids found to have
488 interactions <10% of WT with any of the vTAs. (B) Heat map of the co-IP efficiency of each
489 ORF18 mutant against ORFs 30, 31, and 66.

490

491 **Figure 3**

492 Six ORF18 mutants are consistently defective for interaction with ORF30. (A-D) HEK293T cells
493 were transfected with the indicated vTA plasmids, then subjected to co-IP using α-FLAG beads
494 followed by western blot analysis to detect the ability of WT or mutant ORF18 to interact with
495 ORF30 (*A*), ORF31 (*B*), ORF34 (*C*), and ORF66 (*D*). The co-IP efficiency was calculated as
496 described in the text for 3-4 independent experimental replicates and plotted as bar graphs. In
497 *(A)*, the dotted line represents Y = 0.1, and in *(B-D)*, the dotted line represents Y = 1.0.

498

499 **Figure 4**

500 Impairing the interaction between ORF18 and ORF30 reduces activation of the late K8.1
501 promoter. (A) Diagram depicting the vector combinations that were transfected for the late
502 gene reporter assay. (B) HEK293T cells were transfected with the vTA plasmids including WT or
503 mutant ORF18, the K8.1 or ORF57 promoter reporter plasmids, and the pRL-TK Renilla plasmid
504 as a transfection control. 24 h post-transfection the lysates were harvested and luciferase

505 activity was measured. Data shown are from 3 independent biological replicates, with statistics
506 calculated using an unpaired t-test where (*) $p < 0.05$, (**) $p < 0.005$, and (***) $p < 0.0007$.
507
508 **Figure 5**
509 Disrupting the interaction between ORF18 and ORF30 weakens the assembly of the vTA
510 complex. HEK293T cells were transfected with the indicated vTA plasmids then subjected to co-
511 IP using α-FLAG beads followed by western blot analysis with the indicated antibody. Far right
512 boxed lane is a longer exposure of the ORF18^{E36A_L37A} IP lane. Input represents 2.5% of the
513 lysate used for co-IP. Vinculin was used as a loading control.
514
515 **Figure 6**
516 Characterizing the effect of the E36A_L37A ORF18 mutation on the virus. (A) iSLK cells latently
517 infected with WT KSHV, 18.Stop KSHV, or 18.Stop complemented with ORF18^{WT} or
518 ORF18^{E36A_L37A} were induced to enter the lytic cycle with 1 μg/ml doxycycline and 1 mM sodium
519 butyrate. 72 h post induction, DNA was isolated and fold viral DNA replication was measured by
520 qPCR before and after induction of the lytic cycle. Data shown are from 5 independent
521 biological replicates. (B) Western blots of the expression of the early protein ORF59, the late
522 protein K8.1, ORF18^{WT}, and ORF18^{E36A_L37A} in the indicated cell lines induced as described in (*A*).
523 GAPDH was used as a loading control. (C) HEK293T target cells were spinfected with filtered
524 supernatant from induced cells. Progeny virion production was measured 24 h after
525 supernatant transfer by flow cytometry of GFP+ target cells. Data shown are from 3

526 independent biological replicates with statistics calculated using an unpaired t-test where
527 (****) $p < 0.0001$.
528
529 **Figure 7**
530 Mutating E48_L49 in UL79 disrupts its interaction with UL91. (A) MUSCLE multiple sequence
531 alignment for HCMV UL79 and homologs showing the location of conserved amino acids that
532 correspond to E36_L37 in KSHV ORF18. (B) HEK293T cells were transfected with the indicated
533 plasmids, then subjected to co-IP using α-FLAG beads followed by western blot analysis with
534 the indicated antibody. To normalize for the difference in expression of pUL91 in the different
535 transfection conditions, the co-IP efficiency was multiplied by the fold expression of pUL91 in
536 the presence of WT pUL79 versus E48A_L49A UL79. Input represents 2.5% of lysate used for co-
537 IP. Vinculin was used as a loading control.
538

Table 1. Primer sequences used in this study

Primer Number	Purpose	Sequence 5' - 3'	Orientation
1	ORF18 (L29A)	CATGTGGCGCTTTTTGCAAAATAAGAATGCAAATACATTCCACGCCCAAG	F
2	ORF18 (L29A)	CTTGGGCGTGGAATGTATTTGCATTCTTATTTTGCAAAAAGCGCCACATG	R
3	ORF18 (E36A)	AATACATTCCACGCCCAAGCGCTGCGTTTTATTCATTTG	F
4	ORF18 (E36A)	CAAATGAATAAAACGCAGCGCTTGGGCGTGGAATGTATT	R
5	ORF18 (L37A)	GAACCAAATGAATAAAACGCGCCTCTTGGGCGTGGAATGTAT	F
6	ORF18 (L37A)	ATACATTCCACGCCCAAGAGGCGCGTTTTATTCATTTGGTTC	R
7	ORF18 (N63A)	GGGAGGCTACTGCCGCTGCCGGGACCTACG	F
8	ORF18 (N63A)	CGTAGGTCCCGGCAGCGGCAGTAGCCTCCC	R
9	ORF18 (G65A)	CTCGTCGTAGGTCGCGGCATTGGCAGT	F
10	ORF18 (G65A)	ACTGCCAATGCCGCGACCTACGACGAG	R
11	ORF18 (L72A)	GAACCTTGCGTCCCGCGACCACCTCGTCGT	F
12	ORF18 (L72A)	ACGACGAGGTGGTCGCGGGACGCAAGGTTC	R
13	ORF18 (R74A)	CGCAGGAACCTTGGCTCCCAGGACCACC	F
14	ORF18 (R74A)	GGTGGTCCTGGGAGCCAAGGTTCCTGCG	R
15	ORF18 (K75A)	GGTCCTGGGACGCGCGGTTCCTGCGGAG	F
16	ORF18 (K75A)	CTCCGCAGGAACCGCGCGTCCCAGGACC	R
17	ORF18 (W81A)	TCGTACACGAGCTTCGCCACCTCCGCAGGAAC	F
18	ORF18 (W81A)	GTTCCTGCGGAGGTGGCGAAGCTCGTGTACGA	R
19	ORF18 (Y85A)	TCCTCGAGCCCATCGGCCACGAGCTTCCACAC	F
20	ORF18 (Y85A)	GTGTGGAAGCTCGTGGCCGATGGGCTCGAGGA	R
21	ORF18 (L107A)	GTTCAAGTGCATCCAGGCGCTGTCCCGGTATGCC	F
22	ORF18 (L107A)	GGCATACCGGGACAGCGCCTGGATGCACTTGAAC	R
23	ORF18 (G130A)	GTCGTGGGTGACCGCTAGCCGGTGAAA	F
24	ORF18 (G130A)	TTTCACCGGCTAGCGGTCACCCACGAC	R
25	ORF18 (G145A)	CAGATTAAACAAAAAGTTTGCGTCCACCAGGTTTTCCG	F
26	ORF18 (G145A)	CGGAAAACCTGGTGGACGCAAACTTTTTGTTTAATCTG	R
27	ORF18 (N146A)	TTCCCAGATTAAACAAAAAGGCTCCGTCCACCAGGTTTTCCG	F
28	ORF18 (N146A)	CGGAAAACCTGGTGGACGGAGCCTTTTTGTTTAATCTGGGAA	R
29	ORF18 (L151A)	GAGCACACTTCCCGCATTAAACAAAAAGTTTCCGTCCACC	F
30	ORF18 (L151A)	GGTGGACGGAAACTTTTTGTTTAATGCGGGAAGTGTGCTC	R
31	ORF18 (G152A)	TGCAGGGGAGCACACTTGCCAGATTAAACAAAAAG	F
32	ORF18 (G152A)	CTTTTTGTTTAATCTGGCAAGTGTGCTCCCCTGCA	R
33	ORF18 (R158A)	CGCAAGGAGCAGCGCGCAGGGGAGCACA	F
34	ORF18 (R158A)	TGTGCTCCCCTGCGCGCTGCTCCTTGCG	R
35	ORF18 (L159A)	CGCCGCAAGGAGCGCCCTGCAGGGGAGC	F
36	ORF18 (L159A)	GCTCCCCTGCAGGGCGCTCCTTGCGGCG	R
37	ORF18 (W170A)	ATCGCTGCCCGCAAAGGCGAGGCAGTAGCCC	F

38	ORF18 (W170A)	GGGCTACTGCCTCGCCTTTGCGGGCAGCGAT	R
39	ORF18 (G171A)	CGTGTTCATCGCTGGCCCAAAAGGCGAGG	F
40	ORF18 (G171A)	CCTCGCCTTTTGGGCCAGCGATGAACACG	R
41	ORF18 (E176A)	GCGCACCCAGCGTGCGTGTTCATCGCT	F
42	ORF18 (E176A)	AGCGATGAACACGCACGCTGGGTGCGC	R
43	ORF18 (R180A)	CTGGGCGAAGAAGGCCACCCAGCGTTCG	F
44	ORF18 (R180A)	CGAACGCTGGGTGGCCTTCTTCGCCCAG	R
45	ORF18 (L191A)	AAGACGCCCGGAGACTATCGCGTAGCAAATGAAAAGCTTC	F
46	ORF18 (L191A)	GAAGCTTTTCATTTGCTACGCGATAGTCTCCGGGCGTCTT	R
47	ORF18 (G214A)	CCTCCACCGGAGCGGGATAGCCC	F
48	ORF18 (G214A)	GGGCTATCCCGCTCCGGTGGAGG	R
49	ORF18 (G228A)	GCATACGTTCGTATGGCGTACATGGAGCGGA	F
50	ORF18 (G228A)	TCCGCTCCATGTACGCCATACGAACGTATGC	R
51	ORF18 (E36A_L37A)	CAGAGAACCAAATGAATAAAACGCGCCGCTTGGGCGTGGAATGTATTTAAAT	F
52	ORF18 (E36A_L37A)	ATTTAAATACATTCCACGCCCAAGCGGCGCGTTTTATTCATTTGGTTCTCTG	R
53	ORF18 (R74A_K75A)	CCTCCGCAGGAACCGCGGCTCCCAGGACCACCTCGTC	F
54	ORF18 (R74A_K75A)	GACGAGGTGGTCCTGGGAGCCGCGGTTCCTGCGGAGG	R
55	ORF18 (G145A_N146A)	CTTCCCAGATTAAACAAAAAGGCTGCGTCCACCAGGTTTTCCGGGG	F
56	ORF18 (G145A_N146A)	CCCCGGAAAACCTGGTGGACGCAGCCTTTTTGTTTAATCTGGGAAG	R
57	ORF18 (L151A_G152A)	AGGGGAGCACACTTGCCGCATTAAACAAAAAGTTTCCGTCCACCA	F
58	ORF18 (L151A_G152A)	TGGTGGACGGAAACTTTTTGTTTAATGCGGCAAGTGTGCTCCCCT	R
59	ORF18 (R158A_L159A)	CCGCCGCAAGGAGCGCCGCGCAGGGGAGCACAC	F
60	ORF18 (R158A_L159A)	GTGTGCTCCCCTGCGCGGCGCTCCTTGCGGCGG	R
61	ORF18 (W170A_G171A)	GTGTTCATCGCTGGCCGCAAAGGCGAGGCAGTAGCC	F
62	ORF18 (W170A_G171A)	GGCTACTGCCTCGCCTTTGCGGCCAGCGATGAACAC	R
63	pLVX-TetOneZeo	TTTTTGGAGGCCTAGGCTTTTGCAAAACGCGACCATGGCCAAGTTGACCAGTGC	F
64	pLVX-TetOneZeo	ATTGTTCCAGACGCGTTCAGTCCTGCTCCTCGGC	R
65	2xStrep-ORF34 pCDNA4	GAGAAGGGGGCGGCCTTTGCTTTGAGCTCGCTCGTGT	F
66	2xStrep-ORF34 pCDNA4	AAACGGGCCCTCTAGTTAGAGTTGGTTGAGTCCATTCTCCTTGATC	R
67	UL79-3xFLAG pCDNA4	TACCGAGCTCGGATCATGATGGCCCGCGACG	F
68	UL79-3xFLAG pCDNA4	CTCCCTCGAGCGGCCCCACGTCGTTAGCCAGCGT	R
69	UL91-2xStrep pCDNA4	TACCGAGCTCGGATCATGAACTCGTTGCTGGCGG	F
70	UL91-2xStrep pCDNA4	CTCCCTCGAGCGGCCCTGTCACAGGCGCCCGAG	R
71	ORF18^{WT} and ORF18^{E36A_L37A} pLVX TetOneZeo	CCCTCGTAAAGAATTATGCTCGGAAAATACGTGTGTGAGACC	F
72	ORF18^{WT} and ORF18^{E36A_L37A} pLVX TetOneZeo	GAGGTGGTCTGGATCTTAAACGGGCCCCTTGTCGTCG	R
73	UL79^{E48A_L49A}-3xFLAG pCDNA4	ATGAGGCGTACGATCTTGGCTGCTTCCAAACGCAGCGAGC	F
74	UL79^{E48A_L49A}-3xFLAG pCDNA4	GCTCGCTGCGTTTGGAAGCAGCCAAGATCGTACGCCTCAT	R
75	ORF59 promoter qPCR	AATCCACAGGCATGATTGC	F
76	ORF59 promoter qPCR	CACACTTCCACCTCCCCTAA	R

77	GAPDH promoter qPCR	TACTAGCGGTTTTACGGGCG	F
78	GAPDH promoter qPCR	TCGAACAGGAGGAGCAGAGACCGA	R

Figure 1

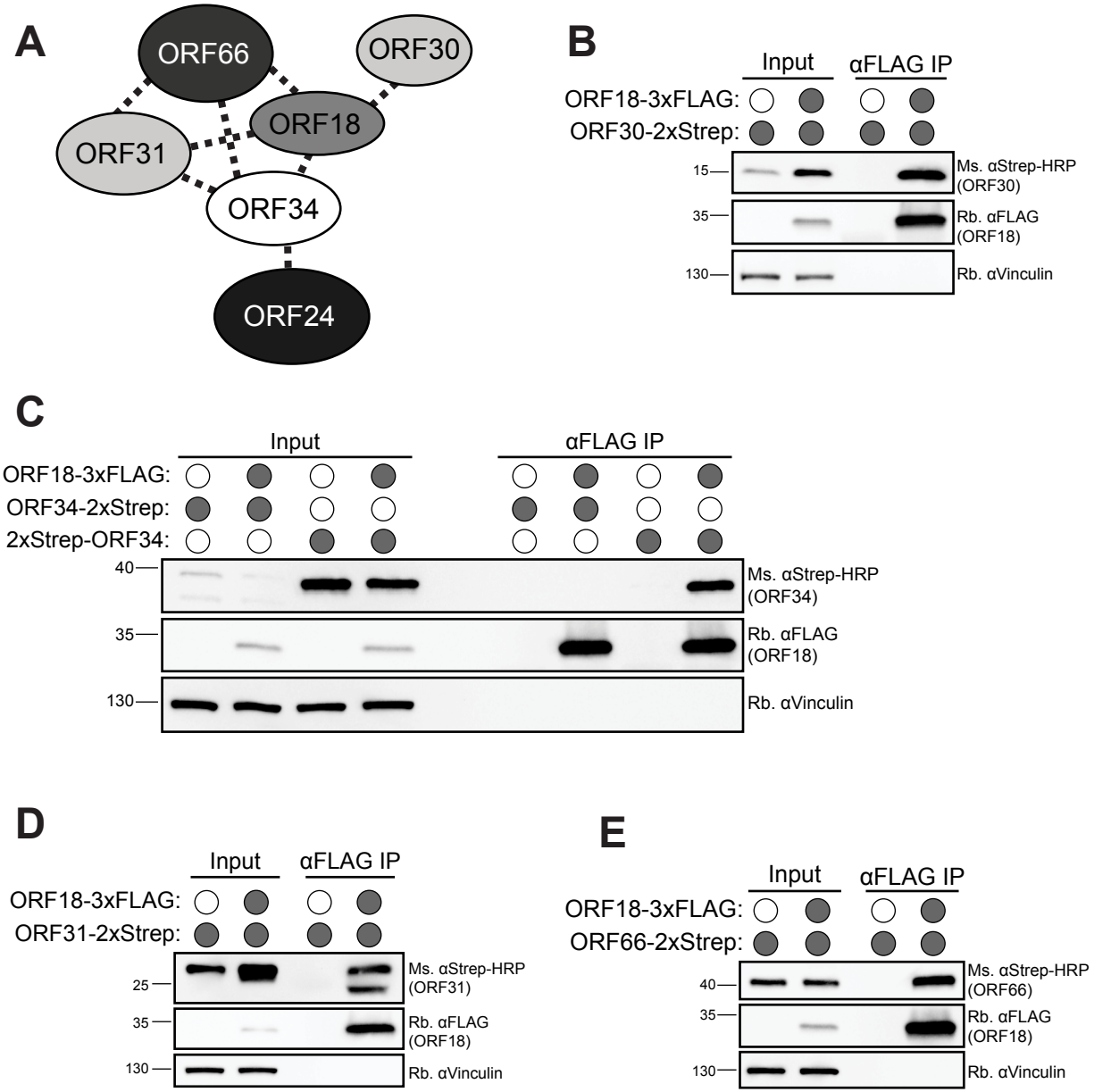
A
ORF66
ORF30
ORF18
ORF31
ORF34
ORF24
B
Input
αFLAG IP
ORF18-3xFLAG:
ORF30-2xStrep:
15
35
130
Ms. αStrep-HRP (ORF30)
Rb. αFLAG (ORF18)
Rb. αVinculin
C
Input
αFLAG IP
ORF18-3xFLAG:
ORF34-2xStrep:
2xStrep-ORF34:
40
35
130
Ms. αStrep-HRP (ORF34)
Rb. αFLAG (ORF18)
Rb. αVinculin
D
Input
αFLAG IP
ORF18-3xFLAG:
ORF31-2xStrep:
25
35
130
Ms. αStrep-HRP (ORF31)
Rb. αFLAG (ORF18)
Rb. αVinculin
E
Input
αFLAG IP
ORF18-3xFLAG:
ORF66-2xStrep:
40
35
130
Ms. αStrep-HRP (ORF66)
Rb. αFLAG (ORF18)
Rb. αVinculin

Figure 2

A

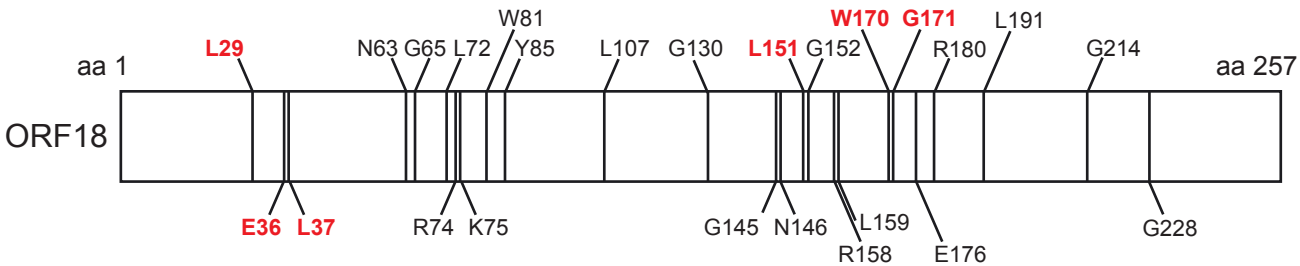
aa 1
aa 257
ORF18
L29
N63 G65 L72
W81
Y85
L107
G130
L151 G152
W170 G171
L191
R180
G214
E36 L37
R74 K75
G145 N146
L159
R158
E176
G228

B

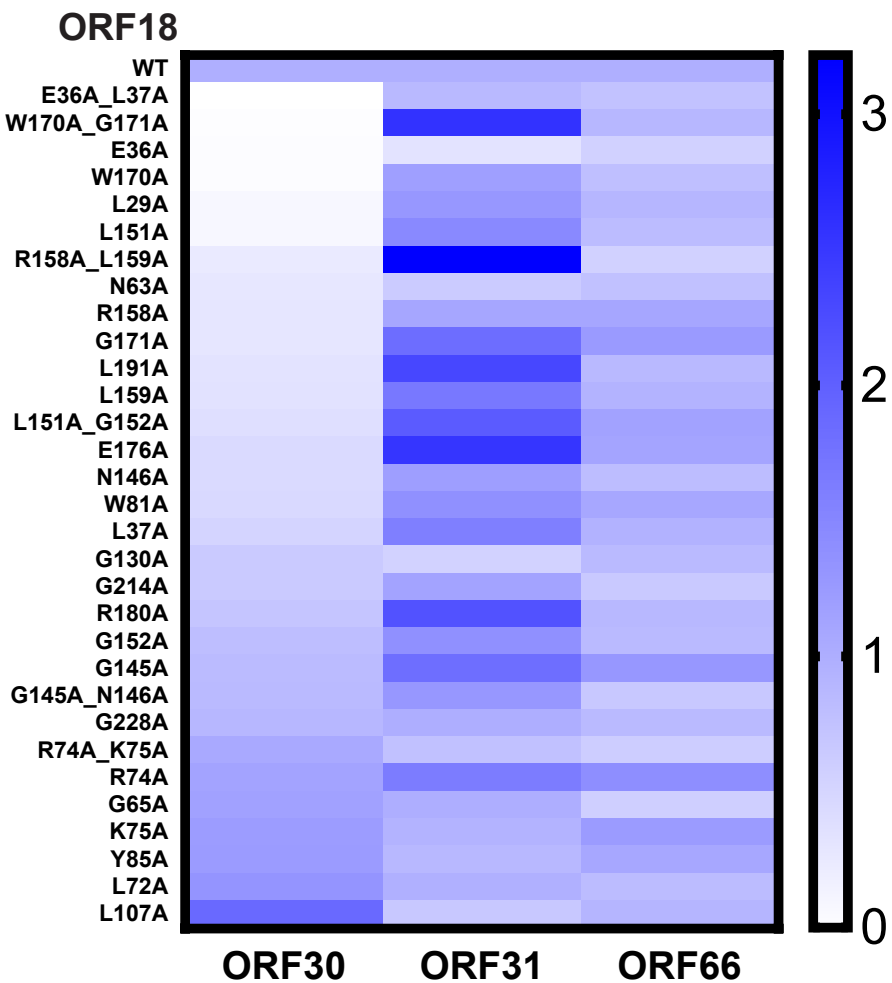
ORF18
WT
E36A_L37A
W170A_G171A
E36A
W170A
L29A
L151A
R158A_L159A
N63A
R158A
G171A
L191A
L159A
L151A_G152A
E176A
N146A
W81A
L37A
G130A
G214A
R180A
G152A
G145A
G145A_N146A
G228A
R74A_K75A
R74A
G65A
K75A
Y85A
L72A
L107A
ORF30
ORF31
ORF66
3
2
1
0

Figure 3

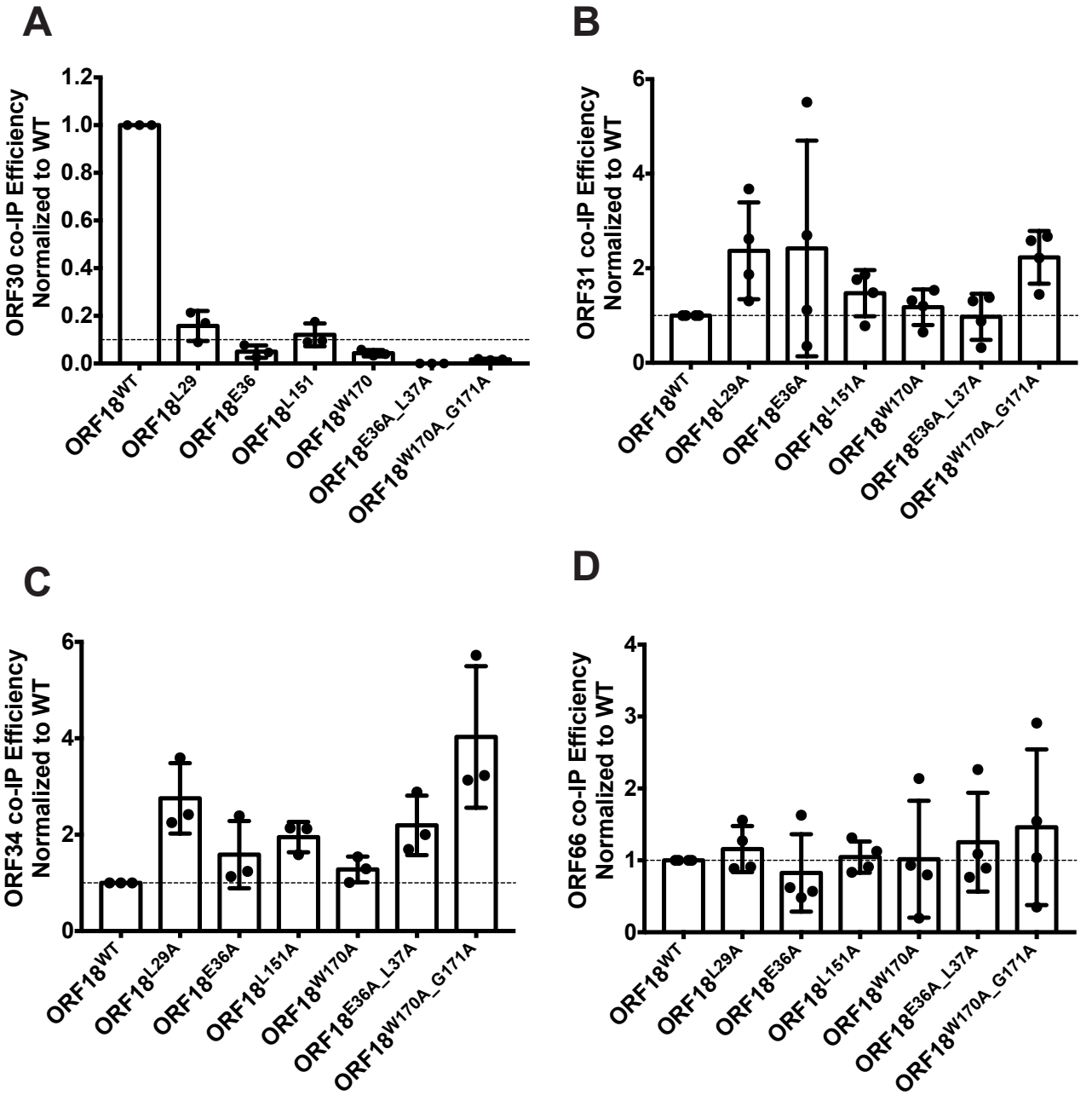
A
ORF30 co-IP Efficiency Normalized to WT
1.2
1.0
0.8
0.6
0.4
0.2
0.0
ORF18WT
ORF18L29
ORF18E36
ORF18L151
ORF18W170
ORF18E36A_L37A
ORF18W170A_G171A
B
ORF31 co-IP Efficiency Normalized to WT
6
4
2
0
ORF18WT
ORF18L29A
ORF18E36A
ORF18L151A
ORF18W170A
ORF18E36A_L37A
ORF18W170A_G171A
C
ORF34 co-IP Efficiency Normalized to WT
6
4
2
0
ORF18WT
ORF18L29A
ORF18E36A
ORF18L151A
ORF18W170A
ORF18E36A_L37A
ORF18W170A_G171A
D
ORF66 co-IP Efficiency Normalized to WT
4
3
2
1
0
ORF18WT
ORF18L29A
ORF18E36A
ORF18L151A
ORF18W170A
ORF18E36A_L37A
ORF18W170A_G171A

Figure 4

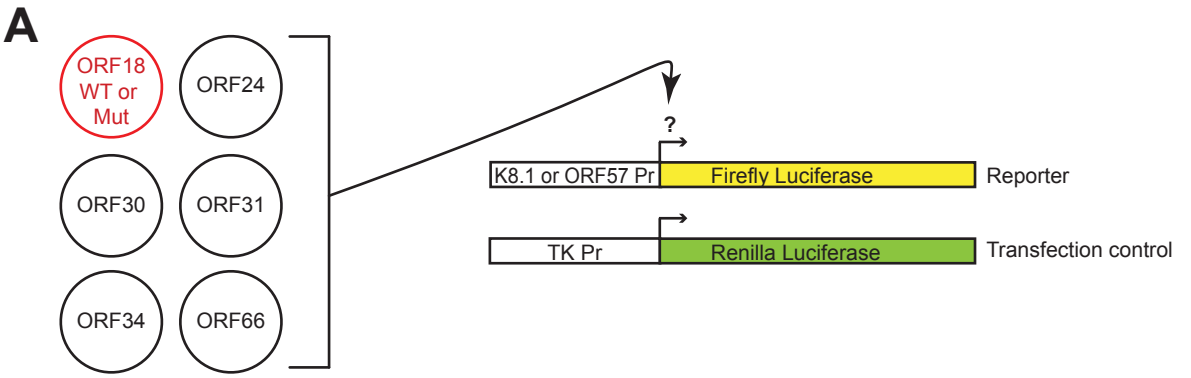
A
ORF18 WT or Mut
ORF24
ORF30
ORF31
ORF34
ORF66
?
K8.1 or ORF57 Pr
Firefly Luciferase
Reporter
TK Pr
Renilla Luciferase
Transfection control

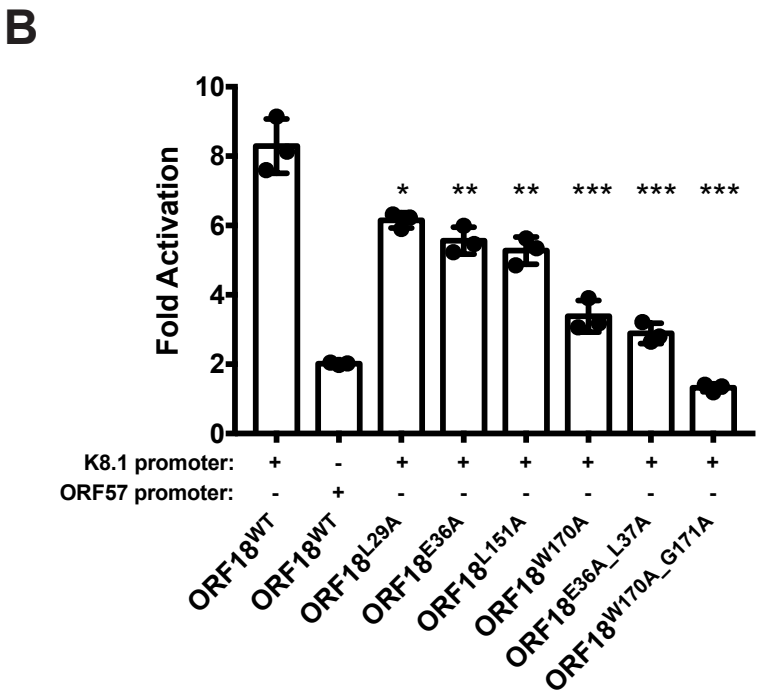
B
Fold Activation
10
8
6
4
2
0
*
**
**
***
***
***
K8.1 promoter: + - + + + + + +
ORF57 promoter: - + - - - - - -
ORF18WT
ORF18WT
ORF18L29A
ORF18E36A
ORF18L151A
ORF18W170A
ORF18E36A_L37A
ORF18W170A_G171A

Figure 5

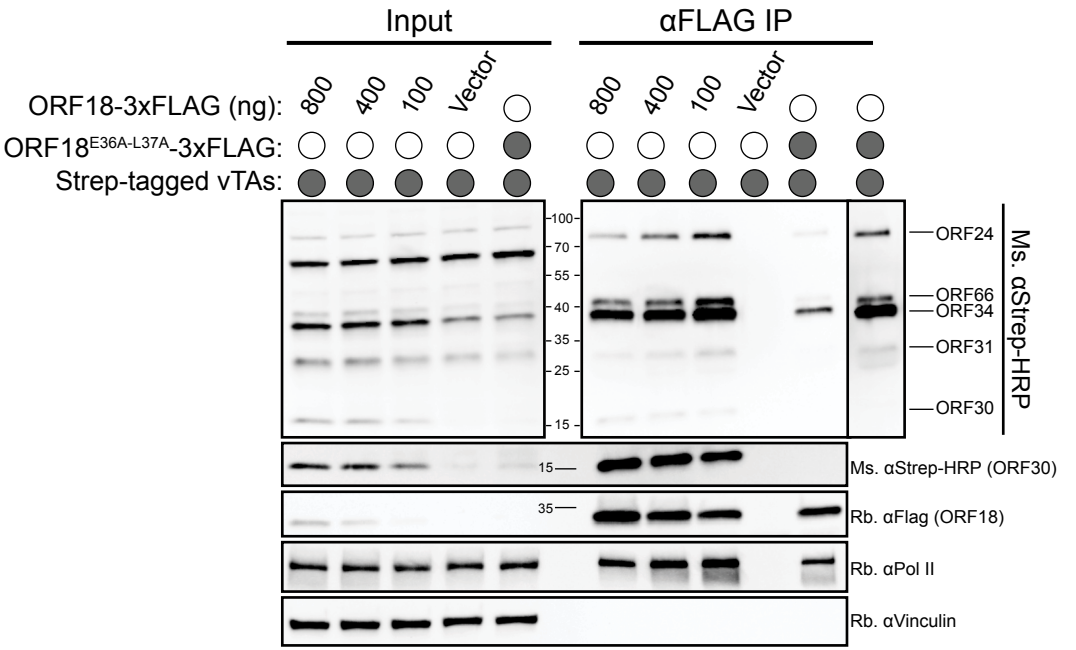
Input
αFLAG IP
ORF18-3xFLAG (ng):
800
400
100
Vector
800
400
100
Vector
ORF18E36A-L37A-3xFLAG:
Strep-tagged vTAs:
100
70
55
40
35
25
15
ORF24
ORF66
ORF34
ORF31
ORF30
Ms. αStrep-HRP
15
Ms. αStrep-HRP (ORF30)
35
Rb. αFlag (ORF18)
Rb. αPol II
Rb. αVinculin

Figure 6

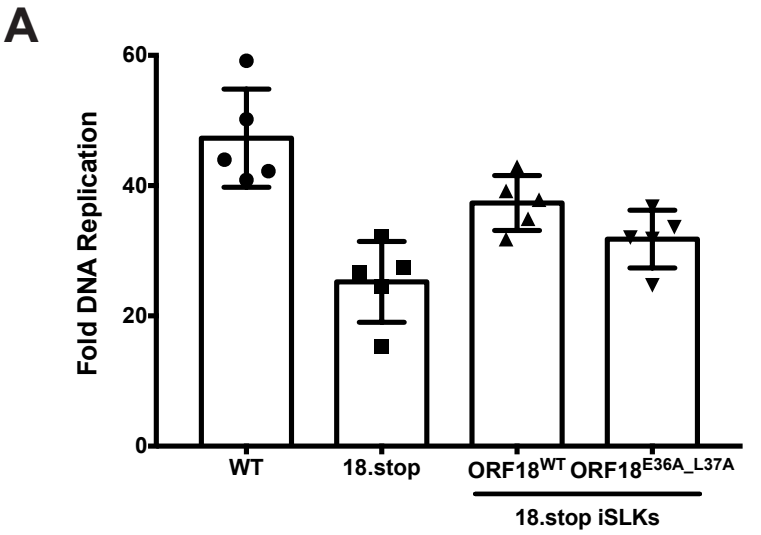
A
Fold DNA Replication
60
40
20
0
WT
18.stop
ORF18WT
ORF18E36A_L37A
18.stop iSLKs

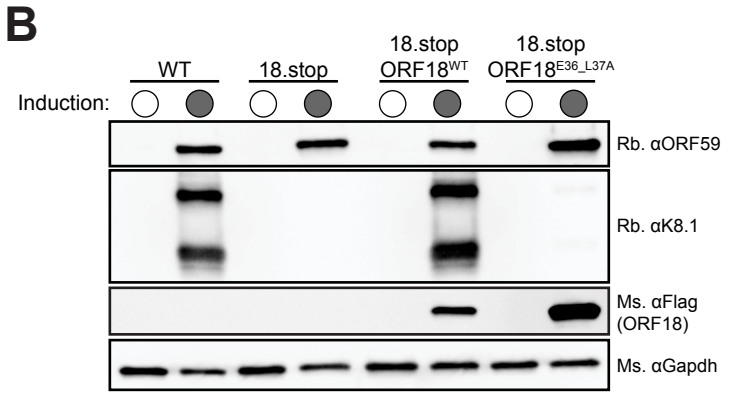
B
WT
18.stop
18.stop ORF18WT
18.stop ORF18E36_L37A
Induction:
Rb. αORF59
Rb. αK8.1
Ms. αFlag (ORF18)
Ms. αGapdh

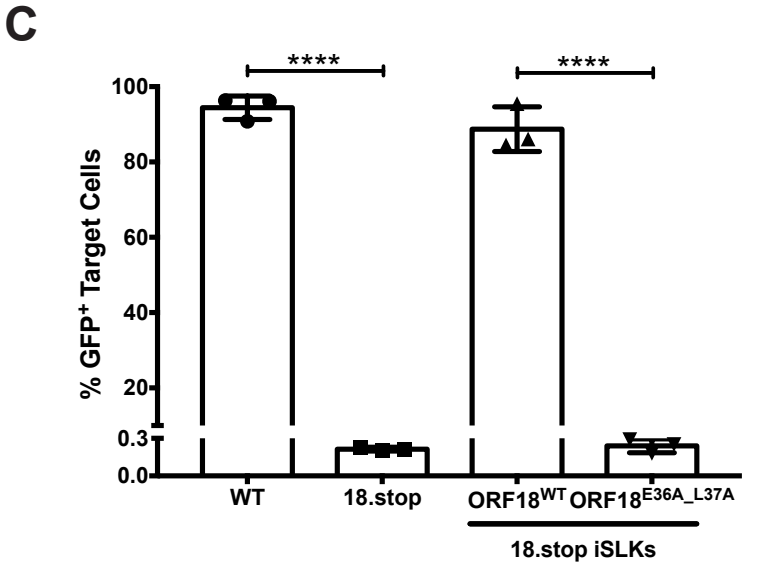
C
% GFP+ Target Cells
100
80
60
40
20
0.3
0.0
****
****
WT
18.stop
ORF18WT
ORF18E36A_L37A
18.stop iSLKs

Figure 7

A

HCMV pUL79	$_{40}$LSSLRLE**EL**KIVRLIC$_{57}$
MCMV pM79	$_{32}$LSSMRLE**EL**KIIRLAC$_{49}$
EBV BVLF1	$_{50}$LCALRED**EL**RFLHLSL$_{67}$
KSHV ORF18	$_{28}$LNTFHAQ**EL**RFIHLVL$_{44}$
MHV68 ORF18	$_{41}$LNTLSST**EL**RLLHAIL$_{58}$
BHV ORF18	$_{28}$LNTYTDE**EL**KFTHMVL$_{44}$
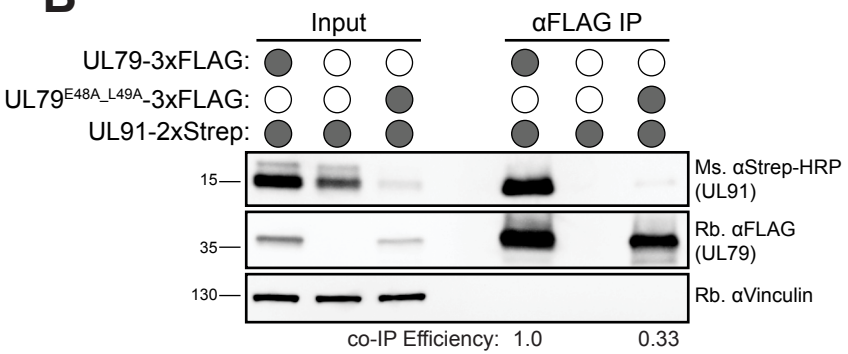
B